REPORT No. 312

THE PREDICTION OF AIRFOIL CHARACTERISTICS

By GEORGE J. HIGGINS

Langley Memorial Aeronautical Laboratory

REPORT No. 312

THE PREDICTION OF AIRFOIL CHARACTERISTICS

By GEORGE J. HIGGINS

SUMMARY

This paper describes and develops methods by which the aerodynamic characteristics of an airfoil may be calculated with sufficient accuracy for use in airplane design. These methods for prediction are based on the present aerodynamic theory and on empirical formulas derived from data obtained in the N. A. C. A. variable density wind tunnel at a Reynolds Number corresponding approximately to full scale.

INTRODUCTION

Since the time that Eiffel first developed the use of the wind tunnel for obtaining the aerodynamic characteristics of airfoils, a great amount of data has been accumulated. Many attempts have been made in the analysis of these data to generalize and thereby develop a method for the prediction of airfoil characteristics. These have been more or less successful. In all cases though, the experimenters have been handicapped by "scale effect." This unknown factor undoubtedly contributed a great deal to the differences found between the models and the full scale wings.

In theoretical aerodynamics, the air is treated as a nonviscous fluid. Consequently, the profile drag of an airfoil can not be accounted for. However, by assuming that the fluid outside of the "boundary layer" is nonviscous and that within the "layer" is viscous, one can combine the pure theory fairly well with the experimental modifications and obtain satisfactory results. Scale effect, also a factor caused by viscosity, can not be determined by theoretical treatment.

Empirical derivations from test data modified in accordance with the above theories lead to certain formulas which may be used for determining airfoil characteristics. Heretofore such expressions have been rather unreliable because of the scale effect mentioned above. Now, however, there are available results of tests made under conditions of full scale on airfoils in the variable density wind tunnel of the National Advisory Committee for Aeronautics. These data then can be used for developing more accurate expressions for prediction.

This paper covers the development of such expressions from experiments in the variable density tunnel and from the present aerodynamic theory. A comparison is made showing the differences between predicted airfoil characteristics and observed data from tests in the wind tunnel at 20 atmospheres density at a Reynolds Number corresponding to full scale.

The author acknowledges the suggestions and aid given in the development of this paper by E. N. Jacobs and M. Knight, of the Langley Memorial Aeronautical Laboratory.

THE PREDICTION OF AIRFOIL CHARACTERISTICS

The main characteristics of an airfoil section are the lift coefficient, profile drag coefficient, and the pitching moment coefficient for any angle of attack within the flying range. When these characteristics are known, any other derived characteristics may be determined and sufficient data is then available for use in airplane design. Heretofore, it has been necessary to use wind-tunnel tests for the particular airfoil to obtain these characteristics. This has been particularly true in regard to the profile drag coefficient because of the lack of theory to cover its computation. Test data from the ordinary wind tunnel have been also subject to correction for scale effect; but there are now available considerable data from tests in the variable density

wind tunnel made at a Reynolds Number equivalent to full scale. Where the term "full scale" is used throughout this report a Reynolds Number of approximately 3,400,000 (a Vl of 534, or a 7¼-foot chord at 50 M. P. H.) is meant.

It is possible to determine the lift and moment coefficients by theoretical computation and the profile drag coefficient by an empirical derivation for any angle of attack up to the burble point. The values of total C_D, L/D, C_p, etc., can then be computed.

The useful angular range in lift from zero lift to the burble point has been found from tests in the variable density tunnel to vary from 18° for thin low cambered sections to 24° for thick high-cambered sections. As a normal airplane is limited to about 15° in its range of angle of attack from the high-speed condition to that of landing, it may be seen that only in special designs does an airplane land or take off at or very near the burble point. Hence, if an airfoil section of normal shape is to be used, the burble point is of secondary importance.

THE LIFT COEFFICIENT

The slope of C_L curve.—Prandtl, Munk, and others, in their development of the theory of lift for an airfoil of infinite span, find the following:

$$C_L = 2\pi \sin \alpha \tag{1}$$

or

$$C_L = 2\pi\alpha \text{ (radians), approx. (Reference 1).}$$

and

$$\frac{dC_L}{d\alpha} = 2\pi \tag{2}$$

For wings of finite span having an elliptical span loading and an aspect ratio of $\frac{b^2}{S}$,

$$\alpha_a = \alpha_e + \alpha_i \tag{3}$$

where α_a = absolute angle of attack measured from the position of zero lift.

α_e = effective angle of attack, i. e., the angle of attack at which an airfoil of infinite span would give the same lift coefficient as the airfoil of finite span under consideration. From equation (1) above,

$$\alpha_e = \frac{C_L}{2\pi}$$

α_i = induced angle of attack.

Munk gives for the induced angle of attack

$$\alpha_i = \frac{C_L S}{\pi b^2} \tag{4}$$

Substituting for α_e and α_i

$$\alpha_a = \frac{C_L}{2\pi} + \frac{C_L S}{\pi b^2} \tag{5}$$

Solving,

$$C_L = \frac{2\pi\alpha_a}{1 + \frac{2S}{b^2}} \quad (\alpha_a \text{ in radians}) \tag{6}$$

$$= 0.10965 \frac{\alpha_a}{1 + \frac{2S}{b^2}} \quad (\alpha_a \text{ in degrees}) \tag{7}$$

Because of the general inefficiency of the wing and because the air is not a nonviscous fluid, experiments show that $\frac{dC_L}{d\alpha_e} < 2\pi$

or

$$\frac{dC_L}{d\alpha_e} = k2\pi \tag{8}$$

From this

$$\alpha_e = \frac{C_L}{k2\pi} \tag{9}$$

The value of k as determined from many tests conducted at a high Reynolds Number in the variable-density wind tunnel is approximately 0.875.

The induced angle of attack is affected by the shape of the plan form. Glauert gives the following expression for the induced angle of attack

$$\alpha_i = \frac{C_L S}{\pi b^2}(1+\tau) \text{ (Reference 2)} \tag{10}$$

where τ is a factor for determining the additional angle caused by the change in span loading from that of the elliptical due to the shape of the plan form. For an elliptical plan form τ is zero. Values for rectangular plan forms of different aspect ratios are given in Table I.

TABLE I

Correction factors for rectangular airfoils

Aspect ratio, $\frac{b^2}{S}$	τ	σ
3	0.11	0.022
4	.14	.033
5	.16	.044
6	.18	.054
7	.20	.064
8	.22	.074
9	.23	.083

Substituting these expressions of α_e and α_i in equation (3) and solving for C_L, one obtains

$$C_L = \frac{2\pi k \alpha_a}{1+\frac{2kS}{b^2}(1+\tau)} (\alpha_a \text{ in radians}) \tag{11}$$

or

$$C_L = \frac{0.0960\alpha_a}{1+\frac{1.75S}{b^2}(1+\tau)} (\alpha_a \text{ in degrees}) \tag{12}$$

The slope of the curve of C_L plotted against α then becomes

$$\frac{dC_L}{d\alpha} = \frac{0.0960}{1+\frac{1.75S}{b^2}(1+\tau)} \tag{13}$$

For an elliptical wing, or a wing having elliptical span loading, of aspect ratio 6.00, where τ is zero,

$$\frac{dC_L}{d\alpha} = 0.0743,$$

and for a rectangular wing of the same aspect ratio

$$\frac{dC_L}{d\alpha} = 0.0714.$$

Angle of zero lift.—

Munk has developed (Reference 3) a method by which the angle of zero lift α_{L_0} may be found. He gives

$$-\alpha_{L_0} = F_1\frac{\xi_1}{c} + F_2\frac{\xi_2}{c} + \cdots\cdots + F_n\frac{\xi_n}{c} \text{ (in degrees)} \tag{14}$$

where

α_{L_0} = angle of attack where the lift is zero, measured from the chord line.

F = a factor.

ξ = ordinates of the mean camber line at a point (X) on the chord line minus the ordinate of the mean camber line at the trailing edge.

c = chord of the airfoil.

For ordinary use, the 5-point method given is sufficiently accurate. This gives

$$-\alpha_{L_0} = 1{,}252.24\frac{\xi_1}{c} + 109.05\frac{\xi_2}{c} + 32.596\frac{\xi_3}{c} + 15.684\frac{\xi_4}{c} + 5.978\frac{\xi_5}{c}, \text{ in degrees} \qquad (15)$$

where ξ_1, ξ_2, etc., are the ordinates of the mean camber line at the points

$$X_1 = 99.458\%\ c$$
$$X_2 = 87.426\%\ c$$
$$X_3 = 50.000\%\ c$$
$$X_4 = 12.574\%\ c$$
$$X_5 = 0.542\%\ c,$$

respectively.

By substituting the correct values in the above equation, the angle of zero lift can be evaluated. Then, knowing that the lift varies very nearly as a linear function of the angle of attack and after determining the slope from equation (13), the curve of C_L vs. α may be readily drawn for the section under consideration. (See fig. 1.) As stated before, the burble

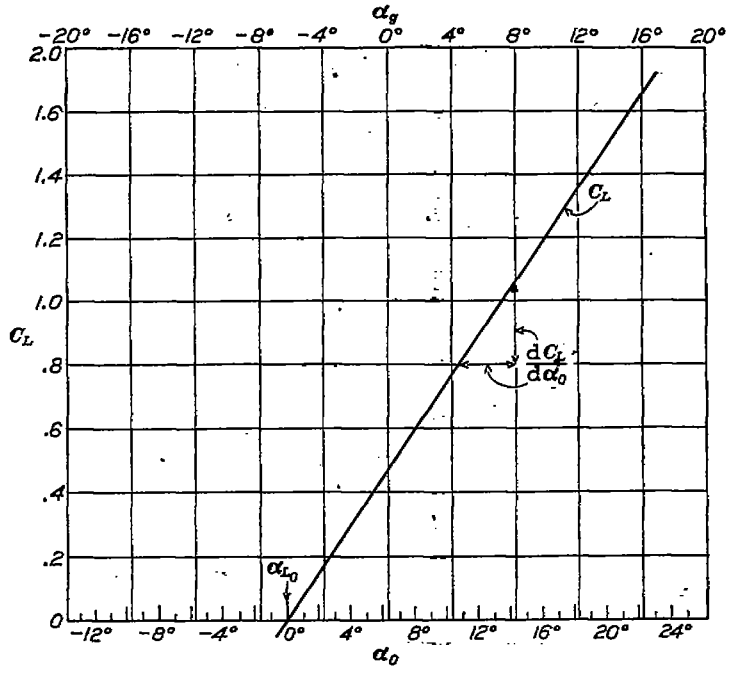

FIGURE 1.—C_L vs. α, α_{L_0} must be determined for each airfoil

point is not known, but this is only of secondary importance. However, it is of interest to note that the highest maximum C_L ever recorded in the variable density wind tunnel on a normal airfoil, i. e., without flaps, slots, etc., at a Reynolds Number equivalent to full scale, is 1.50.

THE DRAG COEFFICIENT

The total drag of a wing may be divided into two parts, the profile drag and the induced drag, or

$$C_D = C_{D_0} + C_{D_i} \qquad (16)$$

Theory gives

$$C_{D_i}=\frac{C_L^2 S}{\pi b^2} \text{ (for elliptically loaded wings, Reference 1)} \tag{17}$$

then

$$C_D=C_{D_0}+\frac{C_L^2 S}{\pi b^2} \tag{18}$$

It has been usually assumed that C_{D_0} is constant for all values of C_L; but from tests on many airfoils at a high Reynolds Number in the variable density tunnel, it appears that this is not the case. Mr. Knight, of the laboratory staff, pointed out that the variation in profile drag for these airfoils was similar and seemed to follow a power law. Let

$$C_{D_0}+=C_{D_{L_0}}\Delta C_{D_0} \tag{19}$$

where $C_{D_{L_0}}$ is the profile drag coefficient when the lift is zero and when there are no disturbances or burbling effects from the lower surface (fig. 2), and where ΔC_{D_0} is the additional profile drag

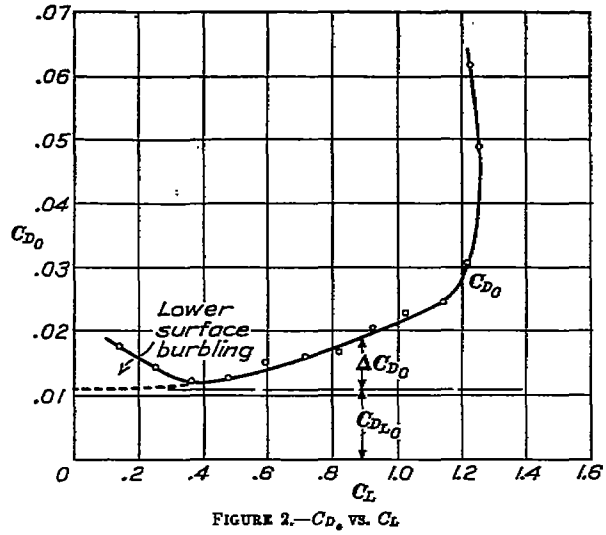

FIGURE 2.—C_{D_0} vs. C_L

coefficient, increasing as the lift increases.

For airfoils that are not extreme in shape and design, values of $C_{D_{L_0}}$ may be found from the charts in Figures 3, 4, and 5. These curves of $C_{D_{L_0}}$ against thickness and against camber

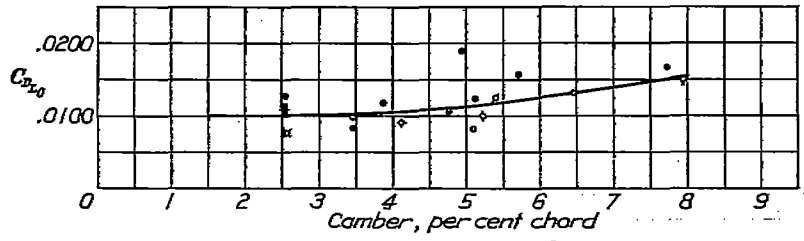

FIGURE 3.—Variation of $C_{D_{L_0}}$ with camber

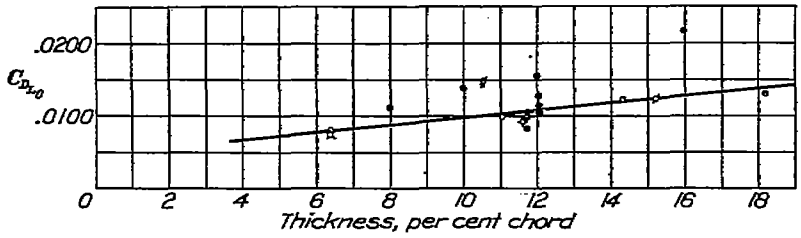

FIGURE 4.—Variation of $C_{D_{L_0}}$ with thickness

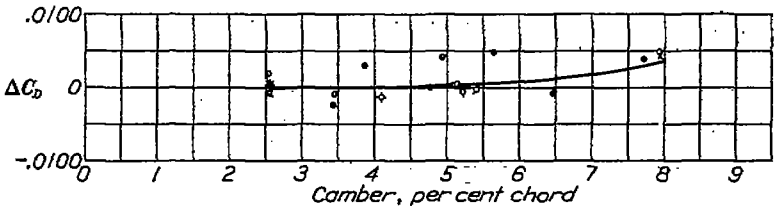

FIGURE 5.—Additional ΔC_D due to the effect of camber

were plotted from data obtained in the variable density tunnel. The accuracy of these curves can be surmised by the scattering of points plotted; the error, however, is only a small per cent of the total wing drag and still a smaller per cent of the total airplane drag.

From Figure 6, where ΔC_{D_o} has been plotted against C_L from 22 tests on different airfoils

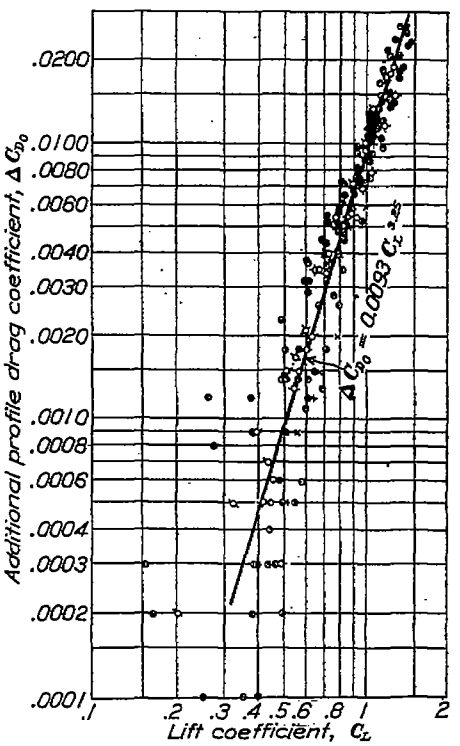

FIGURE 6.—ΔC_{D_o} vs. C_L

at high Reynolds Numbers, one finds in support of Mr. Knight's suggestion that, as a simple approximation

$$\Delta C_{D_o} = 0.0093\ C_L^{3.25} \tag{20}$$

This holds true approximately for all normal-shaped sections. Hence,

$$C_{D_o} = C_{D_{L_o}} + 0.0093\ C_L^{3.25} \tag{21}$$

and

$$\text{Total } C_D = C_{D_{L_o}} + 0.0093\ C_L^{3.25} + \frac{C_L^2 S}{\pi b^2} \text{ (elliptical wings)} \tag{22}$$

$$\text{Total } C_D = C_{D_{L_o}} + 0.0093\ C_L^{3.25} + \frac{C_L^2 S}{\pi b^2}(1+\sigma) \text{ (rectangular wings, Reference 2)} \tag{23}$$

where σ is the factor for the additional induced drag caused by the change in span loading from the elliptical. (See Table I.)

From the above expressions the polar curves can now be determined up to the burble point.

Figure 7 is a chart showing the relationship of the different drag components of a wing or airfoil and of an airplane. The different curves in the upper half of the chart show the effect of aspect ratio and represent the part of the drag that varies with a change in the lift; this portion of the drag is independent of the choice of the section and is equal to the sum of the induced drag and the additional profile drag. The lower part shows the drag dependent on the airfoil section and the other parts of the airplane. This chart is convenient for use for determining rapidly the characteristics of any airfoil section or any airplane.

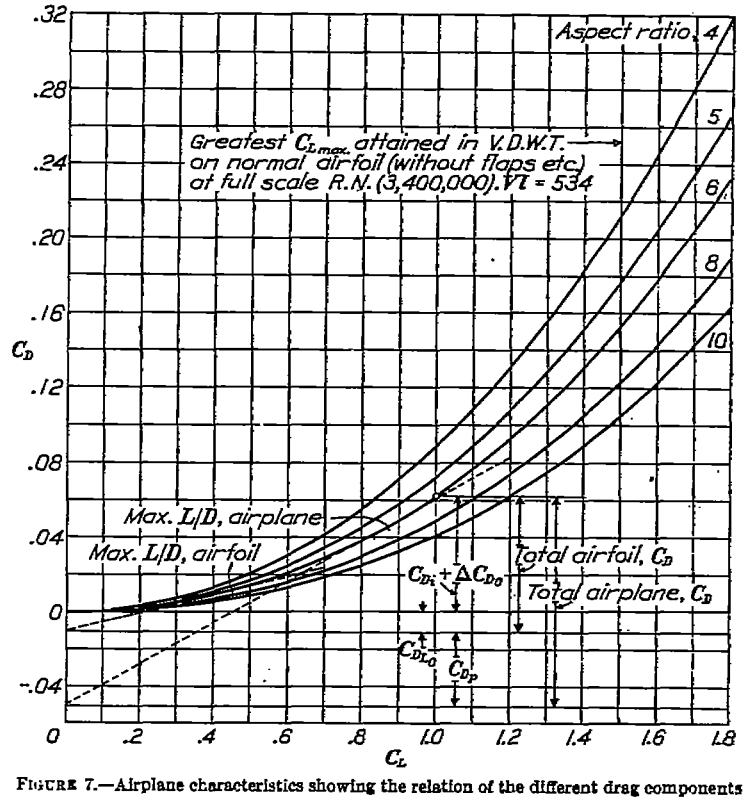

FIGURE 7.—Airplane characteristics showing the relation of the different drag components

LIFT-DRAG RATIO

Values of L/D can be obtained as usual by dividing the C_L by C_D and may be plotted against the angle of attack or the lift coefficient as desired. Values of α, of course, are determined from the curve of C_L vs. α.

THE MOMENT COEFFICIENT

Reference 3 also gives a method for evaluating the angle of attack when the pitching moment about the 50 per cent chord point is zero, α_{M_0}

$$\alpha_{M_0} = 62.634\left(\frac{\xi_A}{c} - \frac{\xi_B}{c}\right), \text{ in degrees} \tag{24}$$

where

ξ = ordinate of the mean camber line at a point (X) on the chord minus the ordinate of the mean camber line at the trailing edge.

$X_A = 95.74\%\ c.$

$X_B = 4.26\%\ c.$

When the airfoil is in such a position that the moment about the 50 per cent point of the chord is zero, the resultant force will obviously pass through this point. Neglecting the moment due to the drag force which is very small, the moment about any other point on the chord can be computed by obtaining the product of the lift force and its lever arm (l) about the point.

(See fig. 8.) By this method, the moment about a point at 25 per cent of the chord is determined. Munk shows theoretically (Reference 1) that the moment about this point is constant for all angles of attack and values of lift. The moment about the quarter chord point becomes

$$M_{c/4}=L_{(\alpha_{M_o})}\times l=L\times\frac{c}{4}\cos\alpha_{M_o}=L\times\frac{c}{4}\text{approximately} \tag{25}$$

and the moment coefficient is

$$C_{M_{c/4}}=\frac{M}{qcS}=\frac{L}{qcS}\times\frac{c}{4}=\frac{C_{L_{(\alpha_{M_o})}}}{4}\quad\text{or}\quad C_{M_{c/4}}=\frac{C_{L_{(\alpha_{M_o})}}}{4}=\frac{1}{4}\times 0.0960\alpha'=0.0240\alpha'. \tag{26}$$

where α' is the angle $\alpha_{L_o}-\alpha_{M_o}$. $C_{M_{c/4}}$ is negative (diving moment) when $C_{L_{(\alpha_{M_o})}}$ is positive. The $C_{M_{c/4}}$ curve may be then plotted by drawing a straight line parallel to the C_L axis and with a $C_{M_{c/4}}$ value as found above.

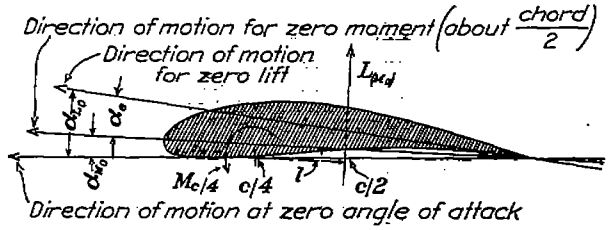

FIGURE 8

CENTER OF PRESSURE COEFFICIENT

The center of pressure coefficient can be readily determined from the other characteristics already computed by the expression

$$C_p=0.25-\frac{C_{M_{c/4}}}{C_L\cos\alpha-C_D\sin\alpha}\quad\text{or}\quad C_p=0.25-\frac{C_{M_{c/4}}}{C_L}\text{, approx.} \tag{27}$$

The latter expression is sufficiently accurate for all general purposes. The graph of C_p vs. C_L can be plotted in the usual manner. It is sometimes convenient to know the C_p in per cent chord aft of the quarter chord point. For this

$$C.\,P.=-100\,\frac{C_{M_{c/4}}}{C_L}\text{, per cent chord.} \tag{28}$$

COMPARISON OF PREDICTED AND OBSERVED CHARACTERISTICS

Figures 9, 10, and 11 show the characteristics of an N. A. C. A. M6 airfoil, a Clark Y airfoil, and an R. A. F. 15 airfoil, all of aspect ratio 6.85 and with a rectangular plan form. There are given on these charts graphs of C_L, C_D, L/D, and $C_{M_{c/4}}$ vs. α, and C_D and C_p vs. C_L. The calculated curves are shown as solid lines and the observed data are shown by points and dashed lines. These latter data are from tests at 20 atmospheres density in the variable density wind tunnel, a Reynolds Number corresponding to full scale. It is interesting to note the close agreement that is obtained between the computed and the observed curves for each of the different characteristics. The greatest difference occurs with the Clark Y section when the characteristics are plotted against the angle of attack. This seems to be mainly as the angle approaches the critical burbling condition. Since the C_D is computed from the C_L, it also is at variance with the observed values in this region. These discrepancies seem to offset each other in the polar curve for there the agreement is good. The predicted L/D curve is slightly low mainly because the observed drag of the Clark Y is low for a section of its thickness.

Figures 12, 13, 14, 15, 16, and 17 show the profile drag coefficients for six common sections, the U. S. A. 35A, N. A. C. A. M6, U. S. A. 27, R. A. F. 15, Clark Y, and the U. S. N. P. S. 4, plotted against C_L. Predicted and observed values are shown here in the same manner. In these charts the C_{D_o} scale is twice the usual one to show the differences more clearly.

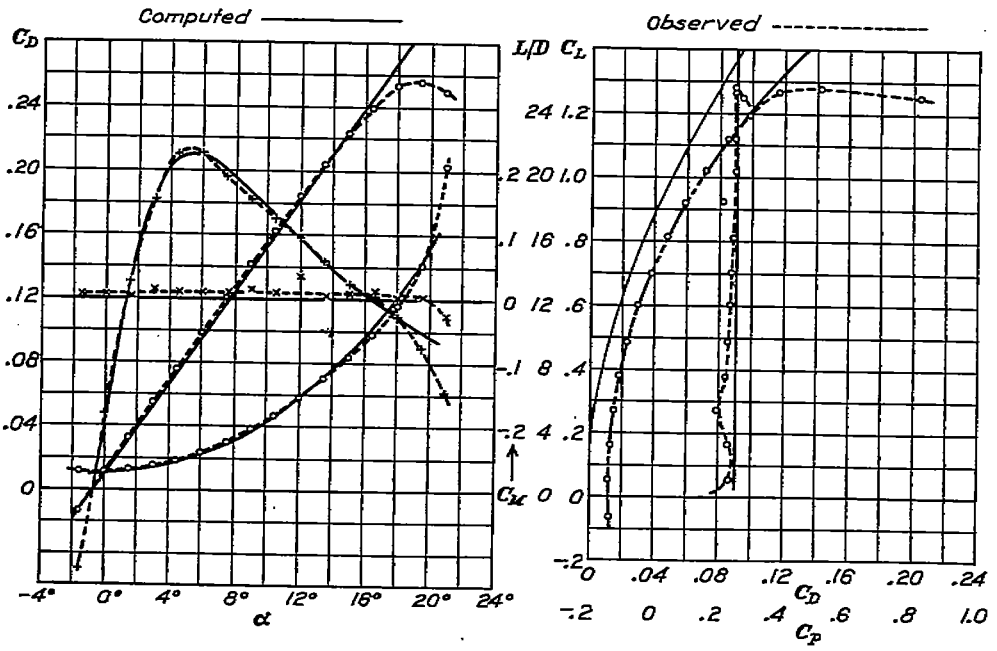

FIGURE 9.—Characteristics of M6 airfoil

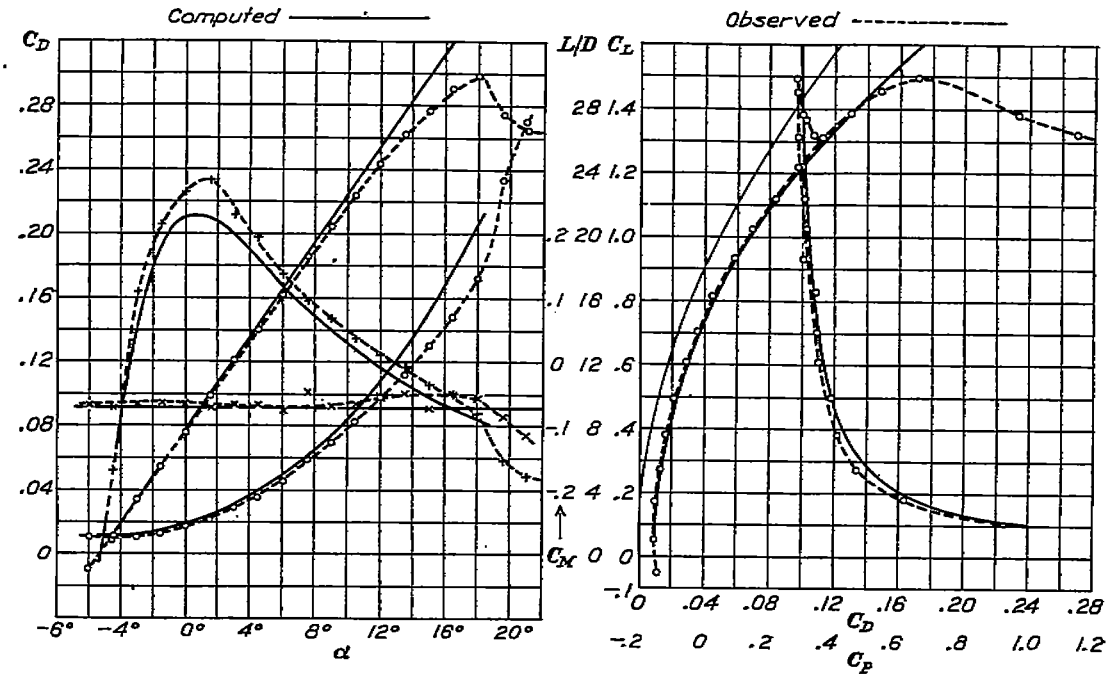

FIGURE 10.—Characteristics of Clark Y airfoil

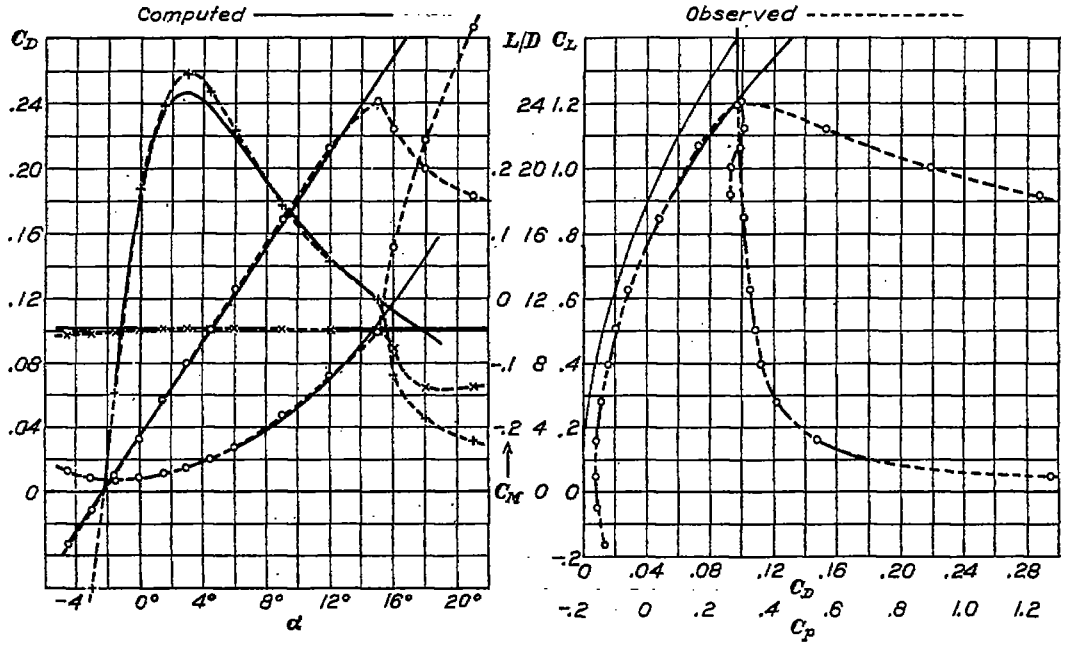

FIGURE 11.—Characteristics of R. A. F. 15 airfoil

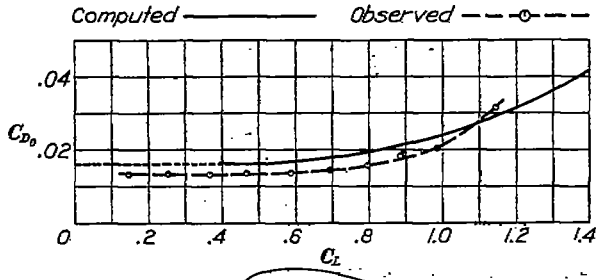

FIG. 12 U.S.A.35A

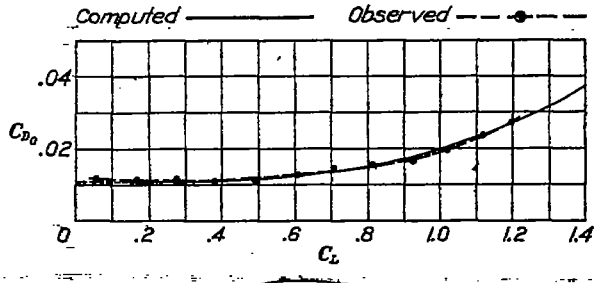

FIG. 13 M 6

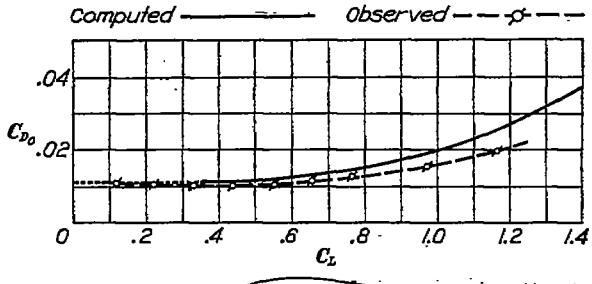

FIG. 14 U.S.A.27

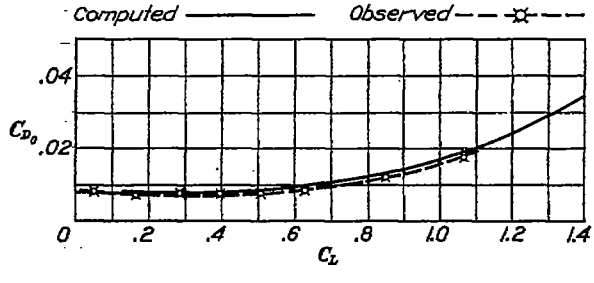

FIG. 15 R.A.F. 15

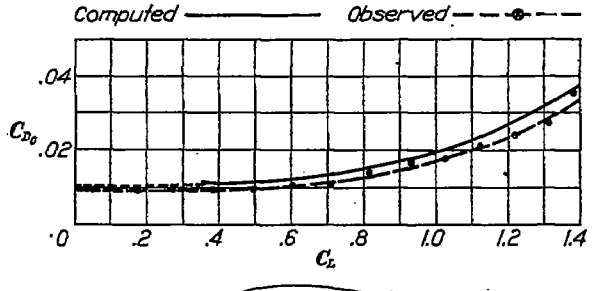

FIG. 16 Clark Y

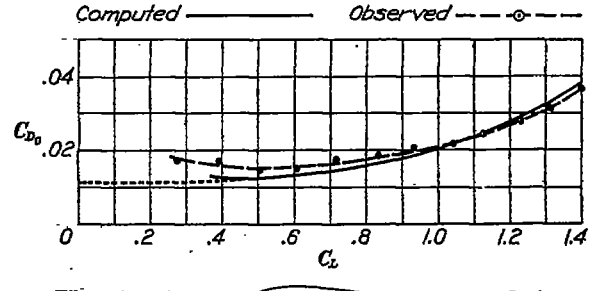

FIG. 17 P.S.4

FIGURES 12, 13, 14, 15, 16, 17.—Profile drag characteristics

CONCLUSION

The aerodynamic characteristics of an airfoil can be predicted by the above methods with sufficient accuracy for use in airplane design. From comparison with observed wind tunnel test data at "full scale" it is found that very close agreement is obtained between the predicted and the actual characteristics from tests.

LANGLEY MEMORIAL AERONAUTICAL LABORATORY,
NATIONAL ADVISORY COMMITTEE FOR AERONAUTICS,
March 14, 1928.

REFERENCES

1. Munk, Max M.: Elements of the Wing Section Theory and of the Wing Theory. N. A. C. A. Technical Report No. 191, 1924.
2. Glauert, H.: The Elements of Airfoil and Airscrew Theory. Chap. XI. Cambridge University Press, 1926.
3. Munk, Max M.: The Determination of the Angles of Attack of Zero Lift and Zero Moment, Based on Munk's Integrals. N. A. C. A. Technical Note No. 122, 1923.

TABLE OF SYMBOLS

C_L	Absolute lift coefficient, L/qS.
$C_{L_{(\alpha_{M_o})}}$	Lift coefficient at the angle α_{M_o}.
C_D	Absolute drag coefficient, D/qS.
C_{D_i}	Induced drag coefficient.
C_{D_o}	Profile drag coefficient.
$C_{D_{L_o}}$	Profile drag coefficient when the lift is zero.
ΔC_{D_o}	Additional profile drag coefficient or $C_{D_o}=C_{D_{L_o}}+\Delta C_{D_o}$.
C_{D_P}	Parasite drag coefficient.
$C_{M_{c/4}}$	Pitching moment coefficient, $\frac{M_{c/4}}{cqS}$.
C_p	Center of pressure coefficient as a fraction of the chord.
$C.\ P.$	Center of pressure.
L	Lift.
D	Drag.
$M_{c/4}$	Pitching moment about the quarter chord point.
L/D	Lift-drag ratio.
α_a	Absolute angle of attack, measured from the position where the lift is zero. (See fig. 1.)
α_i	Induced angle of attack.
α_e	Effective angle of attack.
α_{L_o}	Angle of attack when the lift is zero, measured from the chord line.
α_{M_o}	Effective angle of attack when the moment about the half chord point is zero.
α'	Angle of attack equal to $\alpha_{L_o}-\alpha_{M_o}$.
b	Span of airfoil.
c	Chord of airfoil.
S	Plan form area of airfoil.
q	Dynamic pressure, $\frac{1}{2}\rho V^2$.
ρ	Density of air.
V	Velocity.
k	Correction factor for inefficiency of airfoil. (See text.)
τ	Correction for additional induced angle of attack for rectangular wing.
σ	Correction for additional induced drag coefficient for rectangular wing.
ξ_1, ξ_2, etc.	Ordinates of mean camber line of airfoil at points (X) on chord; for use in determining α_{L_o}.
ξ_A, ξ_B	Ordinates of mean camber line of airfoil at points (X) on chord; for use in determining α_{M_o}.
X_1, X_2, etc.	Points on the airfoil chord. (See text.)
X_A, X_B	Points on the airfoil chord. (See text.)
f_1, f_2, etc.	Multiplying factors. (See text.)